Carpathian Journal of Earth and Environmental Sciences, July 2017, Vol. 12, No. 2, p. 423 - 436

DETERMINISTIC LANDSLIDE SUSCEPTIBILITY ASSESSMENT WITH THE USE OF A NEW INDEX (FACTOR OF SAFETY INDEX) UNDER DYNAMIC SOIL SATURATION: AN EXAMPLE FROM DEMİRCİKÖY WATERSHED (SİNOP / TURKEY)

Mustafa Can CANOĞLU

Sinop University, Faculty of Engineering and Architecture, Environmental Engineering Department, TR-57000 Sinop, Turkey, mccanoglu@sinop.edu.tr

Abstract: Landslides are important natural hazard in Turkey especially in Black Sea Region considering the economic damages and life loss. Sinop city enlarge through hillslope areas with its increasing population. The study area is located in Demirciköy Watershed approximately 11 km southwest of Sinop city centre which embodies several landslides. The aim of the work presented in this paper is to propound a new index representing the deterministic part of the landslide susceptibility phenomenon in terms of FSI (factor of safety index) under dynamic soil saturation conditions. SMDR (Soil Moisture Distribution and Routing) model is employed to simulate the dynamic soil saturation variations utilizing with the monthly mean meteorological data. The calculated dynamic factor of safety is transformed to the FSI with the use of a statistical evaluation known as likelihood ratio method. The ultimate landslide susceptibility maps obtained with the new proposed method indicate that deterministic approach produce fairly acceptable results in terms of physical explanation of landslide existence. On the other hand, spatiotemporal evaluation of the landslide susceptibility concept augment the accuracy comparing with the conventional landslide susceptibility concept according to the produced high performance and satisfactory results.

Keywords: Deterministic landslide susceptibility, Sinop, infinite slope stability, factor of safety index, dynamic soil saturation variations

1. INTRODUCTION

Landslide assessments have become an important argument for urban development and planning especially in enlarging cities due to the quick increase of population. Turkey is subjected to an influx of refugees in recent years which cause an accelerated augmentation of population. Sinop is an attractive city for people with its beautiful nature, commercial opportunities and fast growing university population. To prevent the unexpected events in Sinop city, such as life loss and economic damages in consequence of uncontrolled urbanisation, landslide susceptibility studies gain importance in recent years. Due to the unclear nature and obscuration of landslide triggering mechanism, it is necessary to assess the landslide susceptibility, particularly if there are elements at risk. On the other hand, a standard procedure and parameter sequence does not exist for the landslide susceptibility analysis. Many researchers used a number of methods and parameter for the landslide susceptibility mapping in literature. Three main well known approaches utilized in the literature can be grouped as Geomorphological (expert based), statistical and deterministic. Discussion of the advantages and disadvantages of these different approaches were discussed by many researchers (for example, Hutchinson, 1995; Leroi, 1996; Van Westen et al., 1997; Aleotti & Chowdhury, 1999; Guzzetti et al., 2000; Carrara et al., 2003, Ercanoğlu, 2005; Ray et al., 2010; Süzen & Kaya, 2012; Yılmaz et al., 2012). The Geomorphological methods which are expert dependent, were popular during 1970's and 1980's (Aleotti & Chowdury 1999). This methods are known as heuristic methods also and utilized by many researchers (Ives & Messereli, 1981; Rupke et. al., 1988; Barredo et al., 2000; Concha-Dimas et al., 2007; Kouli et al., 2010). Important disadvantages of expert dependent

landslide susceptibility techniques are subjectivity of parameter selection and updating the final susceptibility map which changes under dynamic environmental conditions. Due to the subjective nature of geomorphological methods, researchers approach to landslide susceptibility concept from quantitative point of view such as statistical and deterministic methods which can be defined as data dependent techniques.

Last decades, landslide susceptibility studies were realized many researchers with the utilization of statistical methods such as bivariate (Fernandez et al., 2003; He et al., 2003; Lin & Tung 2003; Çevik & Topal 2003, 2004; Süzen & Doyuran 2004a; Gökçeoğlu et al., 2005; Saha et al., 2005; Clerici et al., 2002, 2006; Yılmaz & Yıldırım 2006; Mathew et al., 2007; Conoscenti et al., 2008; Dahal et al., 2008a, b; Magliulo et al., 2008; Yalçın 2008; Yılmaz et al., 2012) and multivariate (Carrara et al., 1991; Ercanoğlu et al., 2004; Süzen & Doyuran 2004a, b; Ayalew & Yamagishi, 2005; Can et al., 2005; Yeşilnacar & Topal 2005; Akgün & Türk 2010; Clerici et al., 2002). Some of these researchers were compared bivariate and multivariate statistical methods in landslide susceptibility concept (Süzen & Doyuran, 2004a; Akgün & Türk, 2010). According to Soeters & Van Westen (1996), in statistical method, the combination of parameters that have led to landslides in the past are determined statistically, and quantitative predictions are made for areas currently free of landslides but where similar conditions exist. However, statistical techniques require the collection of large amounts of data to produce reliable results (Ercanoğlu & Gökçeoğlu, 2004).

Deterministic (physically based) approach of landslide susceptibility concepts are generally consist of a methodology that combines the hydrological model for analysing the pore water pressure and the infinite slope stability model for computing its factor of safety (FOS) (Kim, et al., 2014). Deterministic models have been used extensively since 1990's (Montgomery & Dietrich, 1994; Dietrich & Sitar, 1997; Wilcock et al., 2003). Different deterministic approaches introduced by different researchers (Gökçeoğlu & Aksoy, 1996; Pack et al., 1998; Montgomery & Dietrich, 1994; Crosta et al., 2003; Ray et al., 2010). In General, landslides occurred after the excessive rainfall is expressed by many researchers (e.g. Giannecchini et al., 2012; Ayalew, 1999; Calcaterra et al., 2000). These studies using the FOS as base considers the static conditions and/or the rainfall intensity. But, there are some cases which shows that only water effect triggering the landslide is not excessive rainfall such as Derebaşı Landslide (Canoğlu, 2015). The necessity of the reflection of the dynamic water effect in terms of soil moisture to the deterministic landslide susceptibility concept is clear. In some deterministic landslide studies (eg. Ray et al., 2010; Ray et al., 2011), dynamic distributed physically based hydrological models are utilized to simulate soil moisture in the vadose zone but these hydrological models are based on the infiltration excess runoff phenomenon which consider the rainfall intensity. However, most of the landslides in this region occurred independently from precipitation. In this case, using a hydrologic model which base the saturation excess runoff phenomenon represents more realistically the physical characteristics of landslide triggering. For this purpose, Soil Moisture Distribution and Routing (SMDR) model is employed to determine the spatiotemporal soil moisture variations. The temporal soil moisture distributions is utilized for the calculation of FOS for a specific time with the use of frequency ratio in context of bivariate statistical analysis. The calculation of FOS is determined based on the slope stability model reflecting the landslide susceptibility which directly links vadose zone soil moisture, proposed by Ray et al., (2011). In brief, in this study, bivariate statistical analysis and deterministic approach were integrated in context of an interdisciplinary work to produce a new deterministic index (factor of safety index) in terms of landslide susceptibility concept.

2. GENERAL CHARACTERISTICS OF STUDY AREA

The study area, is located in the Black Sea Region which comprises northern part of Turkey and called as Sinop. The climate is oceanic type with high and distributed rainfall the year round. Summers are warm and humid, winters are cool and damp (Atalay, 1997). The Black Sea is the region which receives the greatest amount of precipitation and is the only region of Turkey that receives high precipitation throughout the year. Snowfall is quite common between the months of December and March, snowing for a week or two, and it can be heavy once it snows. In Sinop city, a number of landslide event is recorded every year. Due the topographic structure, soil type and unstable precipitation regime make this region prone to landslide.

The landslide events in this city have been studied by may researchers (eg. Ertek et al., 1993; Işık et al., 2004; Özdemir, 2005). The selected watershed which is located in Black Sea Region covers an area of 8.71 km^2 and known as

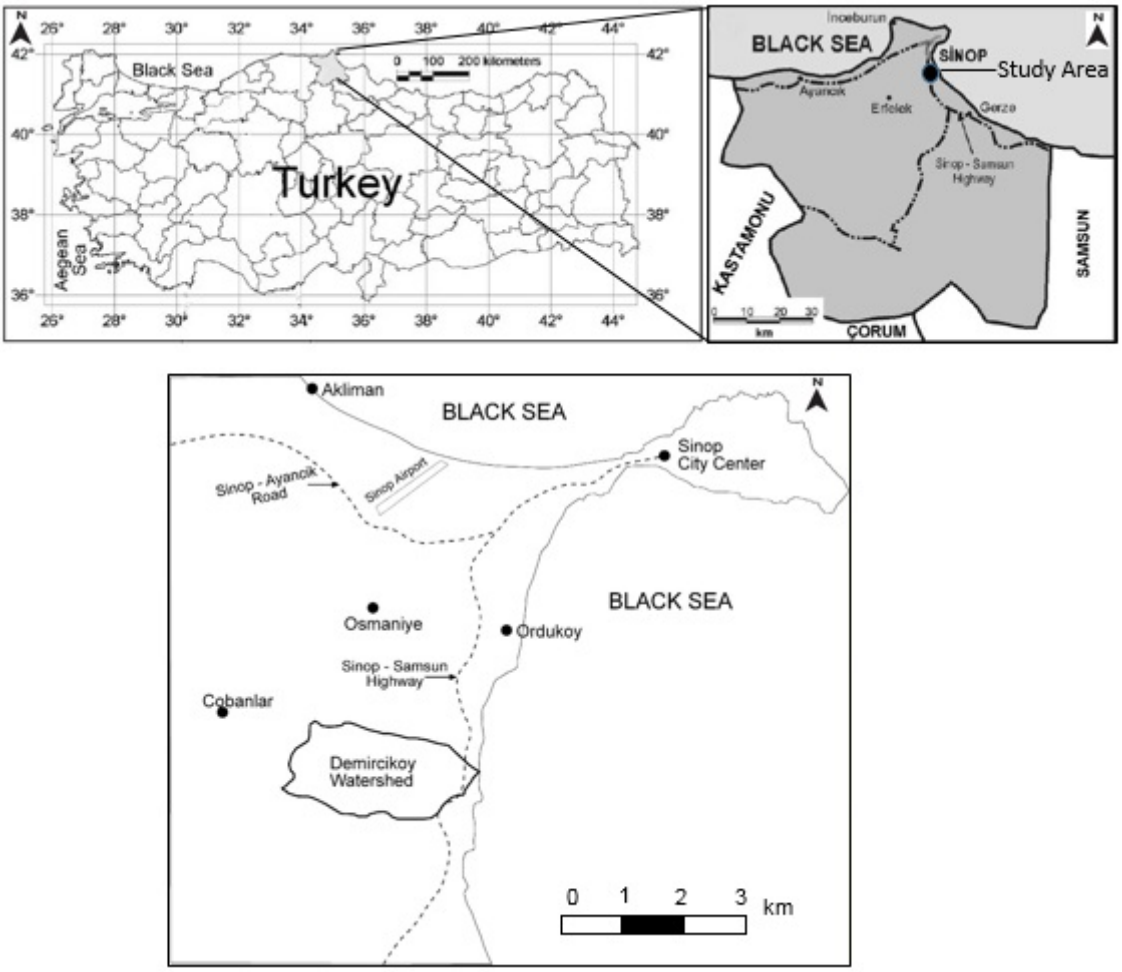

Figure 1: Location map of study area (Demirciköy Watershed)

"Demirciköy Watershed". This Watershed is located 11.2 km southwest of Sinop city centre. The black sea coast road is passing through the Demirciköy Watershed with a tunnel and a viaduct (Fig. 1).

According to Turkish Earthquake Zoning Map prepared by the Earthquake Research Department of the Turkish General Directorate Disaster Affairs, Sinop city is located in the fourth degree earthquake zone. Erdik et al., (1990) mentioned that there is no evidence indicating the presence of active faults in the Sinop city, and there does not exist any potential for surface faulting. Additionally, 0.093 g for 100-year and 0.119 g for 225 year return periods are suggested as a peak horizontal ground accelerations for Sinop city and its near environ by Gülkan et al., (1993). All the seismic arguments show that triggering factor of the landslides in the study area is less probable for earthquakes. Any human activity which can be trigger a landsliding in this region is not recorded. In the present case, water effect is the only dynamic parameter.

Therewithal, landslide occurrence after excessive rainfall is mentioned many researcher as a general expression (e.g. Ayalew, 1999; Calcaterra et al., 2000). However, in some cases (eg. Derebaşı Landslide) the only water effect on landsliding is not excessive rainfall and infiltration characteristics of the soil (Canoğlu, 2015). Under this circumstance, spatiotemporal variation of the soil moisture content is the strong dynamic factor of landsliding in terms of saturation degree. For this reason, to simulate the water effect in vadose zone, SMDR model which is based on the saturation excess runoff phenomenon is employed. A detailed field work is performed in order to determine types, locations, borders and mechanisms of landslides. In the wake of the field works, 6 translational earth slides according to the landslide classification table proposed by Cruden & Varnes (1996) are recorded and mapped (Fig. 2). Stratigraphic situation of the study area and its near environ is formed by the Miocene aged Sinop Formation which is constituted of sandstone, limestone and marl intercalated limestone. The subjected landslides are observed in the weathered part of the Sinop Formation which can be defined as soil type material. Based upon observations, these soil type materials contain predominantly fine grained (silt and clay), small quantity of sand and

trace quantity of gravel. In the Demirciköy Watershed, landslide occurrence depth in the soil horizons varies between 1 m to 5 m, and approximately 3 m in average which indicates shallow landsliding. As from the type and failure mechanism, the landslides observed in the study area are adaptable to the infinite slope stability model.

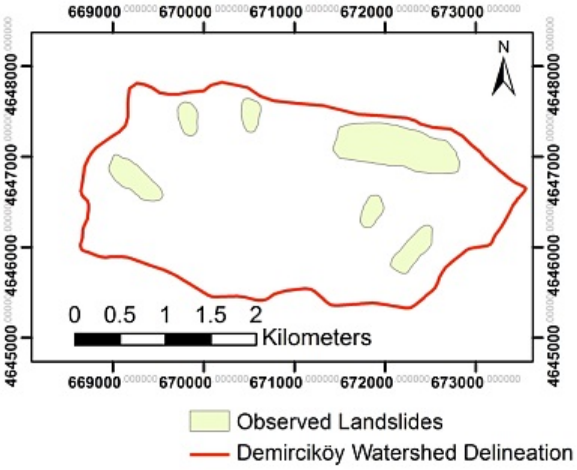

Figure 2: Landslides observed in the study area

Demirciköy Watershed is put out to sea, for this reason the minimum topographic elevation value in the study area is 0 m and maximum is 207 m (Fig. 3a). Slope angles range between 0^o and 21.4^o with an average of 14^o (Fig. 3b). Slope aspect is generally towards the North - Northeast but existence of considerable amount of pixels toward to South is also remarkable (Fig. 3c). Agricultural lands exist in gentle slopes while extensive and thick forests cover the highest and steepest elevations.

3. METHODOLOGY AND INPUT DATA

The aim of this study is to satisfy the lack of a new index for landslide susceptibility concept which represent the physical landsliding mechanism and reflect the water effect in vadose zone in terms of spatiotemporal variations of soil saturation. In line with this objective, a slope stability model (modified by Ray et al., 2010) is utilized to generate FOS map of the study area in which the spatiotemporal variations of soil moisture are determined by SMDR model. Concurrently, to engender the new spatiotemporal and deterministic index called as "Factor of Safety Index" (FOSI) frequency ratio analysis is employed. Finally, monthly mean landslide susceptibility maps of the study area are composed with the use of classical topographical thematic layers and the FOSI obtained from the integrated approach which utilize slope stability model (modified by Ray et al., 2010), SMDR model and frequency ratio analysis.

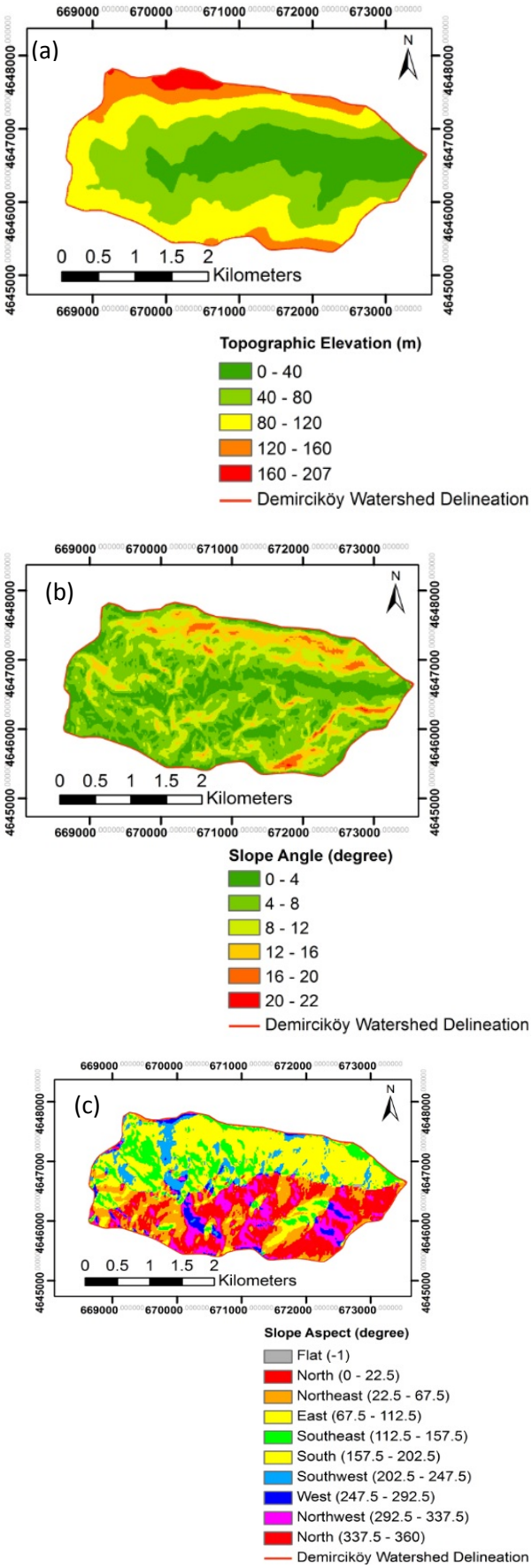

Figure 3: Topographical parameter maps: a) topographical elevation (m); b) slope angle (^{o}); c) slope aspect (^{o})

3.1 Slope Stability Model

Slope stability studies have been performed and analysed to determine the FOS in detailed investigations by many researchers (van Westen and Terlien 1996; Acharya et al. 2006; Ray & De Smedt 2009). In this study, to calculate the FOS infinite slope model introduced by Skempton & DeLory (1957) is based. In slope stability analysis FOS is defined as the ratio of resisting forces to driving forces and expressed by Ray et al., (2010) as a modified version herein below;

$$FOS = \frac{C_s + C_r}{\gamma_e H \sin\theta} + \left(1 - m\frac{\gamma_w}{\gamma_e}\right)\frac{\tan\varphi}{\tan\theta} \quad (1)$$

where C_s and C_r are the effective soil and root cohesion (kN/m^2), γ_e is the effective unit soil weight (kN/m^3), H is the total depth of the soil above the failure plane (m), θ is the slope angle (^{o}), m is the wetness index (dimensionless), φ is the angle of internal friction of the soil (^{o}), and γ_w is the unit weight of water (kN/m^3). The calculation of the effective unit weight is proposed by Ray et al., (2010) as follow;

$$\gamma_e = \frac{q\cos\theta}{H} + (1-m)\gamma_d + m\gamma_s \quad (2)$$

where q is any additional load on the soil surface (kN/m^2), γ_d is dry unit soil weight (kN/m^3) for the unsaturated soil layer, γ_s is the saturated soil unit weight. And the wetness index m follows Ray et al., (2010).

$$m = \frac{h + (H-h)\times S_w}{H} \quad (3)$$

where h is the saturated thickness of the soil (m) above the failure plane and S_w is the saturation degree of soil (cm^3/cm^3) or vadose zone soil moisture.

Ray et al., (2010) categorised the calculated FOS into susceptibility classes based on the stability classification system proposed by Pack et. al., (1998) and Acharya et. al., (2006). Based on this categorisation, four susceptibility classes have been introduced, highly susceptible (FOS≤1), moderately susceptible (1<FOS<1.25), slightly susceptible (1.25<FOS<1.5) and not susceptible (stable) (FOS ≥1.5). But, expressing FOS alone as the landslide susceptibility would be contrarian to the philosophy of the landslide susceptibility concept. Because, landslide susceptibility concept considers probability of potential landslide as the main subject. In contrast, slope stability analysis represent the physical mechanism of a slope failure, so a critical threshold can be talked about when the resisting force equals the sliding force and the FOS = 1. However, transforming FOS into an index and using in landslide susceptibility will represent the process more deterministic.

3.1.1. Input Data of Slope Stability Model

Laboratory tests have been performed in order to determine the parameters utilized in the infinite slope stability model. The average values of these laboratory tests are used due to considering the homogeneity of Demirciköy Watershed ground conditions. Soil cohesion and angle of internal friction values are determined from triaxial compressive strength test as 2,65 kN/m^2 and 15,9^o respectively. Root cohesion value is obtained from Directorate of Sinop Forestry Branch Office as 8 kPa for the specific forestry products of Demirciköy and its near environ. The average values of dry unit soil weight γ_d is 15,4 kN/m^3 and the saturated soil unit weight γ_s is 25,4 kN/m^3. The housing area map and the additional load from the structures (approximately 250 kN/m^2) is handled from Sinop Special Provincial Directorate of Administration. The landslides observed in the study area have all the slip surface above the water table based on the water table map obtained from General Directorate of State Hydraulic Works. So, the saturated thickness of the soil above the failure plane h is 0 m. The soil depth map is obtained from Sinop Provincial Directorate of Agriculture. This map is considered as the depth of the soil above the failure plane. The slope angle "θ" map is generated by spatial analyst tool of the ArcGIS 10 software (ESRI, 2010). Finally the monthly saturation degree "S_w" map is simulated by SMDR model (Soil and Water Laboratory, 2003).

3.2 SMDR Model

Use of geographical information systems in hydrological and hydrogeological modelling have been used to analyse the ground and surface water flux by many studies (Kurtuluş, 2012; Kurtuluş & Flipo, 2012; Kurtuluş & Razack, 2010). But in these studies the interaction between the vadose zone and aquifer is generally rule outed and infiltration excess runoff phenomenon which consider the rainfall intensity becomes prominent. However, in landslide studies using a hydrologic model which base the saturation excess runoff phenomenon represents

more realistically the physical characteristics of landslide triggering. For this purpose, in this study SMDR model is employed in order to determine the saturation degree of soil and its spatiotemporal distribution. SMDR model is a spatially distributed hydrological model produced for vadose zone which base the variable source area concept in terms of saturation excess runoff phenomenon. In this study SMDR model divides the watershed in a square grid cells with cell dimensions 10m x 10m, this dimension mentioned by Boll et al., (1998) as optimal. SMDR model considers precipitation and lateral flow from surrounding upslope cells as input and lateral flow to surrounding down-slope cells, percolation and evapotranspiration as output for the water budget calculation. Water mass balance equation for each cell which represents the water budget calculation is expressed as follow;

$$W^2 |\Theta(t) - \Theta(t - \Delta t)| = |RF(t) + SM(t)| + Qi(t) - Qo(t) - ET(t) - P(t) - SE(t) \quad (4)$$

where W is the (square) grid size (m), Θ the cell average water content ($cm^3.cm^{-3}$), Δt the time step (d), RF and SM the rainfall and snowmelt volumes, respectively, Qi the volume of water received through lateral flow from surrounding upslope cells, Qo the volume of water lost through lateral flow to surrounding downslope cells, ET the volume of water lost by evapotranspiration, P the volume of water lost by percolation and SE the saturation excess runoff. For this study the soil thickness is taken as 1m. Volumes are expressed in (m^3). The daily mean air temperature is corrected by the adiabatic lapse rate of 6.5 x 10^{-3} for the local elevation changing (Boll et al., 1998). Precipitation occurring when the mean daily temperature is below 0°C is assumed to be snow. Snow is assumed to remain until the mean daily temperature is above 0°C. Snowmelt SM is computed following a simple land-cover dependent temperature index method (US Army Corps of Engineers, 1960). The subsurface flow is expressed by Darcy Law where the hydraulic conductivity of the layer (m.day−1) is defined as:

$$\begin{aligned} K(\Theta) &= 0 && \text{for } \Theta < \Theta_f \\ K(\theta) &= K_{sat}.\exp\left(\alpha \frac{(\theta - \theta_s)}{(\theta_s - \theta_f)}\right) && \text{for } \Theta_f \le \Theta < \Theta_m \\ K(\Theta) &= K_m + K_s \frac{(\theta - \theta_m)}{(\theta_s - \theta_m)} && \text{for } \Theta_m \le \Theta \end{aligned} \quad (5)$$

Where, Θ_f, is field capacity, Θ_m is macroporous drainage limit and Θ_s is soil moisture content. $K_s=K(\Theta_s)$ and $K_m=K(\Theta_m)$ are the hydraulic conductivity at saturation and at macroporous drainage limit, respectively. On the other hand, α is a universal constant equal to 13 for a large range of soils (Bresler et al., 1978). Basically the ratio between actual to potential ET increases linearly with water content from zero at or below the permanent wilting point, Θ_{pwp}, to a value of one at or above the evapotranspiration limit, Θ_{etl} (Frey et al., 2009).

Percolation is calculated for each cell as;

$$P = min[K(\Theta); K_{sub}]W^2 \Delta t \quad (6)$$

where K_{sub} is the conductivity at saturation of the cell substratum, (m/day), and where the hydraulic conductivity K is given by Eq. (5). Percolation stops when the average water content of the bottom structural layer is less than field capacity. In the SMDR model, the water more than saturation is added to the amount of runoff.

3.2.1. Input Data of SMDR Model

In order to execute the SMDR model 5 raster maps (topographical elevation map, soil type map, vegetation characteristics map, watershed boundary map and aspect map) and 4 ASCII look-up tables (vegetation characteristics table, soil characteristics table, plant development factor table and daily meteorological table) are required.

E34-a1 named and 1/25000 scaled topographic map (National Mapping Agency of Turkey, 1993) is digitized in order to handle the topographical elevation map of the study area. The horizontal resolution of this map is 10m x 10m. Watershed boundary and aspect maps (Fig. 3c) are generated by spatial analyst tool of the ArcGIS 10 software (ESRI, 2010). Vegetation characteristics map, vegetation characteristics table and plant development factor table are obtained from Directorate of Sinop Forestry Branch Office. Soil characteristics table is compiled based on the laboratory tests (grain size distribution) and estimated from soil texture through statistical relationships proposed by Rawls and Brakensiek (1982; 1985). For this purpose ten representative soil samples have been collected from study area. Subsequently, grain size distribution of the soil samples have been determined with laboratory tests. Based on the laboratory test results, each soil sample is classified according to USDA (United States Department of Agriculture) soil texture classification system (USDA, 1999). According to USDA soil texture classification system the soil type of the study area is homogenous (Fig. 4). For this reason the soil type map represents only one soil type.

Daily meteorological data is obtained from the General Directorate of Meteorological Service of

Turkey for Sinop Station between the years 1975-2010. Monthly mean precipitation, daily temperature, monthly potential evapotranspiration are utilized in the SMDR model.

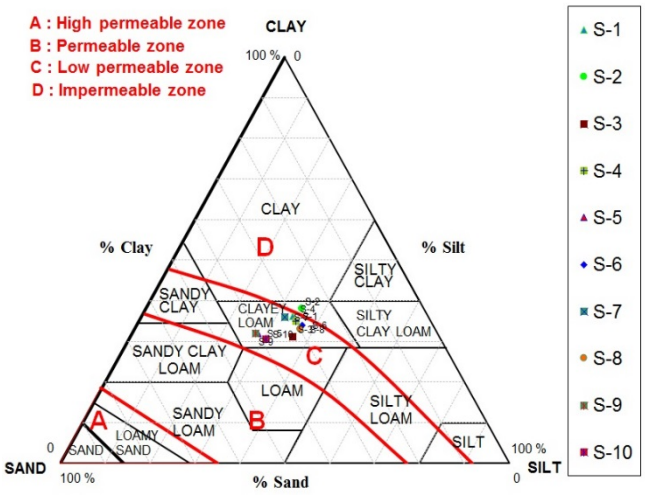

Figure 4: Textural classification of the soil samples in the study area according to USDA soil texture classification system.

"The past and the present are keys to the future" is the principle introduced by Varnes (1984). This principle is interpreted as the landslide causal factors of past should be taken into account for the potential landsliding future. The reflection of the statistical relation between the landslide causal factors and the landslide areas is an important point to clear up the landsliding in the future. For this reason, frequency ratio analysis is selected to reflect the landslide occurrence probability. Frequency ratio is defined as the ratio of occurrence probability to nonoccurrence probability for specific attributes (Bonham-Carter, 1996). Increment of this ratio from 1 refers the strong relationship between the landslide and its causal parameters, conversely, decrement of frequency ratio from 1 attributed the weakness of this relationship. The spatial weighting relationship between the FOS map of each month and landslide frequency ratio values for each FOS classes is determined as shown on table 1.

Sequentially, the parameter maps are converted to the discrete categorical maps to determine the weight of each parameter class as an index map. In this way a new index and its responsible weights for each class can be specified as done in this study to introduce the FOSI. The schematic production procedure of FOSI is shown on figure 5.

Calculation of ultimate landslide susceptibility map is made by the overlaying each parameter's frequency ratio values as in equation 7 and 8. In order to underline the influence of the FOSI in landslide susceptibility concept, only basic topographic parameters are utilized in eq.7 and FOSI is added to basic (elementary) parameters in eq.8.

LANDSLIDE SUSCEPTIBILITY (1) = Fr (Slope) + Fr (Aspect) + Fr (Elevation) (7)

LANDSLIDE SUSCEPTIBILITY (2) = Fr (Slope) + Fr (Aspect) + Fr (Elevation) + Fr (FOSI) (8)

where, LANDSLIDE SUSCEPTIBILITY (1) is landslide susceptibility computed by considering basic topographic parameters, LANDSLIDE SUSCEPTIBILITY (2) is landslide susceptibility computed by considering basic topographic parameters and FOSI computed by annually mean meteorological data (between the years 1975-2010), Fr is frequency of each parameter for each class.

Comparison of two landslide susceptibility maps generated by eq.7 and eq. 8 emphasize the influence of FOSI in terms of accuracy (Fig. 6a and b). In other words, reddish areas become redder and the bluish areas become bluer. Under this circumstance, it can be say that, eq.8 including the FOSI represents the susceptibility more precisely.

Table 1: Spatial relationships between FOS and landslide and its frequency ratio values

PARAMETER	CLASS RANGE	NUMBER OF PIXEL WITHOUT LANDSLIDE	RATIO-a (%)	NUMBER OF PIXEL WITH LANDSLIDE	RATIO-b (%)	FREQUENCY RATIO b/a
FOS OF JANUARY	0-1	7782	10.15	5699	56.67	5.58
	1-1.25	10626	13.86	2188	21.76	1.57
	1.25-1.50	11591	15.11	1033	10.27	0.68
	1.50-1.75	7934	10.35	413	4.11	0.40
	>1.75	38753	50.53	724	7.20	0.14
FOS OF FEBRUARY	0-1	6371	8.31	5673	56.41	6.79
	1-1.25	12098	15.78	2211	21.98	1.39
	1.25-1.50	11648	15.19	1038	10.32	0.68
	1.50-1.75	8018	10.46	420	4.18	0.40
	>1.75	38551	50.27	715	7.11	0.14

FOS OF MARCH	0-1	6452	8.41	5173	51.44	6.11
	1-1.25	10422	13.59	2728	27.13	2.00
	1.25-1.50	11374	14.83	916	9.11	0.61
	1.50-1.75	8707	11.35	484	4.81	0.42
	>1.75	39731	51.81	756	7.52	0.15
FOS OF APRIL	0-1	7735	10.09	5676	56.44	5.60
	1-1.25	10645	13.88	2422	24.08	1.73
	1.25-1.50	11581	15.10	846	8.41	0.56
	1.50-1.75	10072	13.13	399	3.97	0.30
	>1.75	36653	47.80	714	7.10	0.15
FOS OF MAY	0-1	6462	8.43	5145	51.16	6.07
	1-1.25	10453	13.63	2751	27.35	2.01
	1.25-1.50	11571	15.09	925	9.20	0.61
	1.50-1.75	8526	11.12	482	4.79	0.43
	>1.75	39674	51.74	754	7.50	0.14
FOS OF JUNE	0-1	7698	10.04	5548	55.17	5.50
	1-1.25	10663	13.90	2529	25.15	1.81
	1.25-1.50	11585	15.11	938	9.33	0.62
	1.50-1.75	10021	13.07	327	3.25	0.25
	>1.75	36719	47.88	715	7.11	0.15
FOS OF JULY	0-1	7724	10.07	5610	55.78	5.54
	1-1.25	10653	13.89	2480	24.66	1.78
	1.25-1.50	11581	15.10	925	9.20	0.61
	1.50-1.75	10039	13.09	327	3.25	0.25
	>1.75	36689	47.84	715	7.11	0.15
FOS OF AUGUST	0-1	6487	8.46	5131	51.02	6.03
	1-1.25	10428	13.60	2767	27.51	2.02
	1.25-1.50	11545	15.05	930	9.25	0.61
	1.50-1.75	8554	11.15	478	4.75	0.43
	>1.75	39672	51.73	751	7.47	0.14
FOS OF SEPTEMBER	0-1	7688	10.03	5472	54.41	5.43
	1-1.25	10691	13.94	2578	25.63	1.84
	1.25-1.50	11539	15.05	963	9.58	0.64
	1.50-1.75	9994	13.03	408	4.06	0.31
	>1.75	36774	47.95	636	6.32	0.13
FOS OF OCTOBER	0-1	6663	8.69	5139	51.10	5.88
	1-1.25	10518	13.72	2512	24.98	1.82
	1.25-1.50	11526	15.03	1187	11.80	0.79
	1.50-1.75	7164	9.34	437	4.35	0.47
	>1.75	40815	53.22	782	7.78	0.15
FOS OF NOVEMBER	0-1	6623	8.64	5139	51.10	5.92
	1-1.25	10489	13.68	2765	27.49	2.01
	1.25-1.50	11562	15.08	931	9.26	0.61
	1.50-1.75	7166	9.34	434	4.32	0.46
	>1.75	40846	53.26	788	7.84	0.15
FOS OF DECEMBER	0-1	6559	8.55	5140	51.11	5.98
	1-1.25	10442	13.62	2762	27.46	2.02
	1.25-1.50	11551	15.06	929	9.24	0.61
	1.50-1.75	8529	11.12	475	4.72	0.42
	>1.75	39605	51.65	751	7.47	0.14

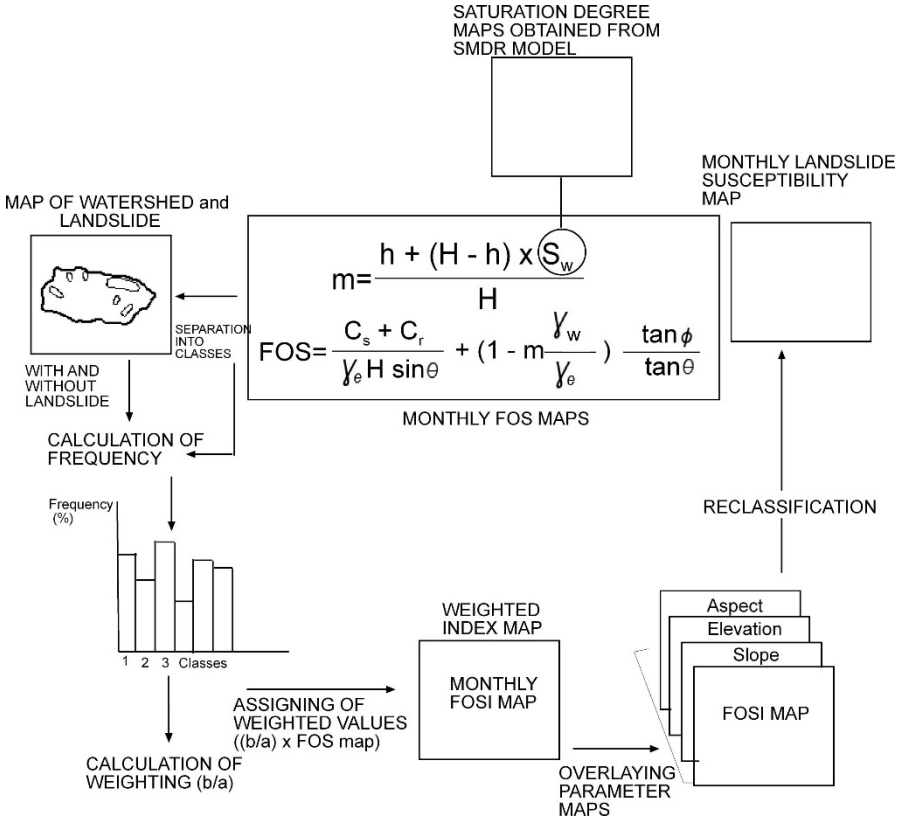

Figure 5. Work flow diagram representing the production of FOSI map in context of landslide susceptibility

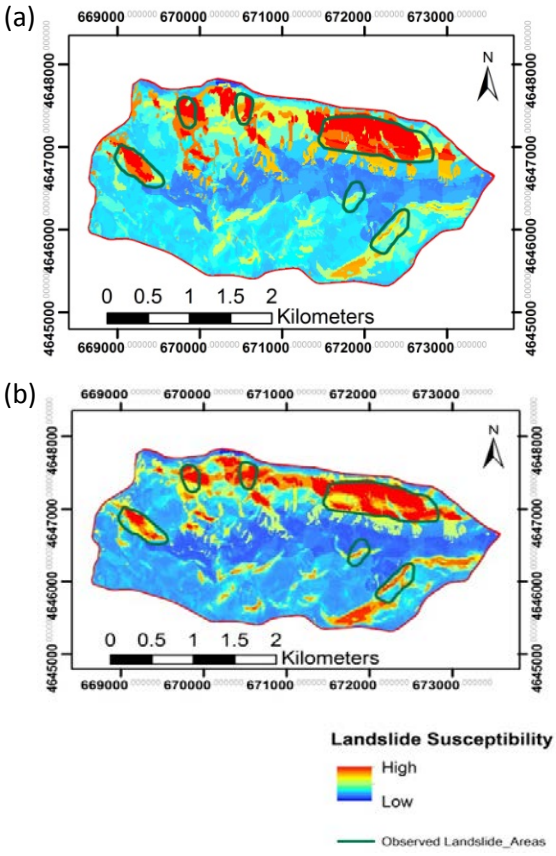

Figure 6: Comparison of Landslide Susceptibility Maps of Demircköy Watershed (a) computed by eq.7, (b) computed by eq.8

Sequentially, in order to generate a mathematical expression including the FOS and FOSI for utilization in landslide susceptibility concept. Factor Of Safety Index (FOSI) chart is composed (Fig. 7) from the Table 2.

Table 2. Spatial relationship between factor of safety and factor of safety index

Factor Of Safety Class	Number of Pixels Without Landslide	Ratio-a (%)	Number of Pixels With Landslide	Ratio-b (%)	Frequency Ratio (b/a)	Factor Of Safety Index
0-1	6371	8.31	5673	56.41	6.79	0.72
1-1.25	12098	15.78	2211	21.98	1.39	0.15
1.25-1.50	11648	15.19	1038	10.32	0.68	0.07
1.50-1.75	8018	10.46	420	4.18	0.40	0.04
>1.75	38551	50.27	715	7.11	0.14	0.02

The equation of the curve on the figure 7 is;

$$FOSI = 3.189e^{-3FOS} \qquad (9)$$

The coefficient of correlation of the equation 9 is 0.94, best fitting FOS-FOSI relationship. However, utilization of this equation for a large scaled watershed can misguide the users. Furthermore, FOSI approach is based upon the infinite slope stability concept and not valid for deeper landslides. More precisely, it is tested that the equation 9 is valid for Demircköy Watershed, but

the general validity of this equation should be investigated for the future studies.

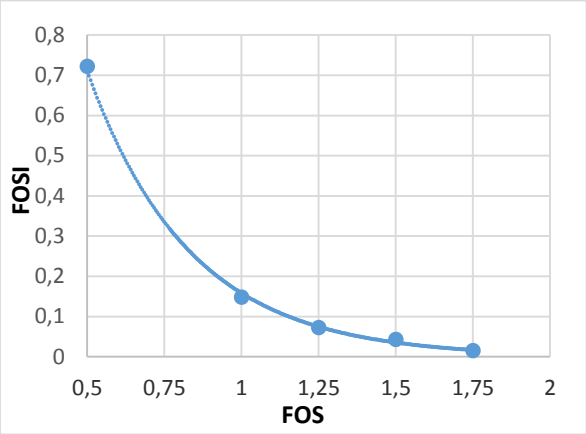

Figure 7. Relationship chart between the factor of safety index and factor of safety

4. RESULTS AND CONCLUSIONS

By favor of this study, a new perspective is presented for the landslide susceptibility concept in order to represent the physical mechanism of landsliding with the integration of Factor of Safety (FOS). A new index called as "Factor of Safety Index" FOSI is generated considering the dynamic soil saturation with the incorporation of infinite slope stability model, variable source area concept and frequency ratio analysis. The following results and conclusions can be drawn from the present study:

a) A new procedure is introduced in order to generate landslide susceptibility map. Under this integrated approach, infinite slope stability model represents the physical mechanisms of landslide occurrence with a factor of safety, SMDR model determine the spatiotemporal variations of soil moisture which is a part of the FOS and frequency ratio analysis is utilized in order to reveal the spatial relationship between FOS and FOSI as the statistical part.

b) İnfinite slope stability model is a conventional technique enlightening the physical processes of landsliding. But, as in some studies utilizing it directly as landslide susceptibility is non compatible with the gist of landslide susceptibility concept. Because, by definition landslide susceptibility is relative spatial probability of potential landslide occurrence on the contrary of slope stability analysis which represents the physical mechanism of a slope failure expressing with a factor named as Factor of Safety (FOS) considering a critical threshold when the resisting forces equal the sliding forces (FOS=1). However, under favor of this study FOS is transformed into an index in order to utilize in landslide susceptibility which represents the physical processes on behalf of determinism.

c) A classical slope stability model fulfil the expectation of a physical failure mechanism for a specific slope. Due to the advancement in the geographic information systems slope stability concept gave the place to landslide susceptibility concept which represent a spatiality within the years. But a temporal representation of a susceptibility study including the physical failure mechanism diminish the uncertainties and bring a deterministic perspective.

d) Considering the seismic records, human activity and excessive rainfall conditions, there is no recorded significant dynamic factor which can trigger a landsliding in this area. For this reason the variation of water fluxes in vadose zone of the study area are analyzed in terms of saturation degree. Using the saturation degree maps within the FOS calculation, satisfies the lack of spatiotemporal effect of physical processes on landslide susceptibility mapping. Furthermore, the integration of FOS into the landslide susceptibility concept which consider the dynamic soil saturation variations underlines the temporal dimension of the landslide susceptibility concept.

e) The basic topographic thematic layers are utilized as inputs of landslide susceptibility mapping. FOSI is added to the basic topographic parameters in order to compare to emphasize the influence of FOSI (Fig. 6a and b). It is seen from figure 6a and b that the transitions between landslide susceptibility classes become sharper with the use of FOSI. Thus it is provided that utilization of FOSI within landslide susceptibility is more effective, determinist and accurate.

f) Finally, landslide susceptibility maps for 12 months are generated from the monthly mean meteorological data as a new method (Fig. 8). These maps indicate that the most susceptible months are April and June for Demirciköy Watershed. This integrated approach achieve the goal of a better representation of physical failure mechanism in context of diminishing the uncertainties of landslide susceptibility. Figure 6a and b is also substantiate the validity of this proposed method. Additionally, %88 of areal extent of the actual landslides exist in the very high susceptibility zone with the use of FOSI.

g) This deterministic method representing the physical failure mechanism within landslide susceptibility can be applied for the local scaled which incorporate at least one landslide. This method should be developed for the watersheds which

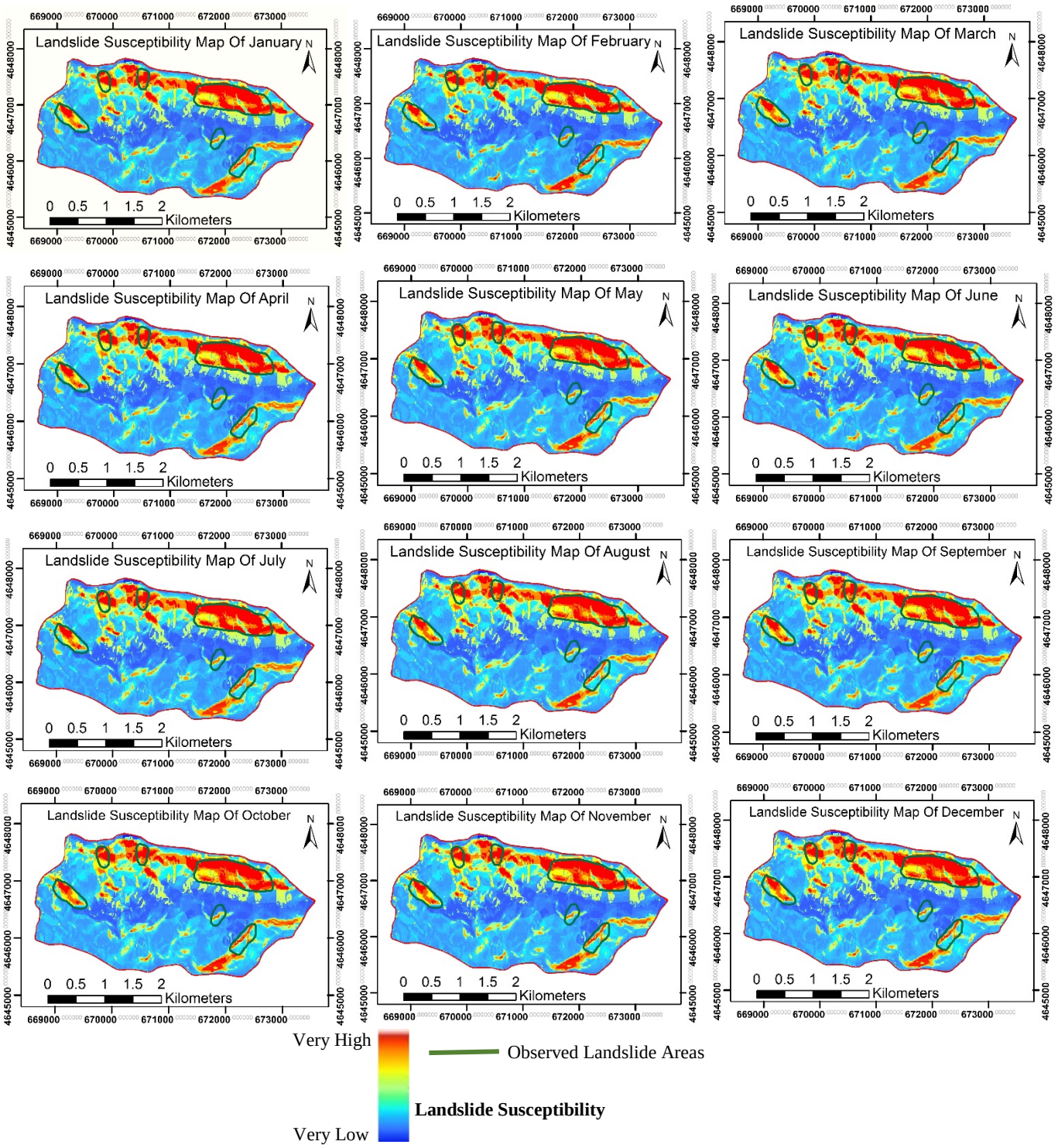

Figure 8: Spatial patterns of monthly landslide susceptibility produced with FOSI in Demirciköy Watershed

does not embody any landslide and for different scales in the name of the future research studies.

h) One of most important problem in landslide susceptibility mapping is selection of suitable parameter and determination of their weighting. It is believed that, with this study the lack of physical failure representation is satisfied and a new index is introduced into landslide susceptibility concept on behalf of determinism. However, with regard to the definition of susceptibility, the map obtained using with this method is not certain and should not be utilized for design purposes. The main advantage of this method is to go a step further through the truth.

REFERENCES

Acharya, G., De Smedt, F. & Long, N. T., 2006. *Assessing landslide hazard in GIS: a case study from Rasuwa, Nepal.* Bulletin of Engineering Geology and the Environment, 65(1), 99–107.

Akgün, A. & Türk, N., 2010. *Comparison of Bivariate and*

Multivariate Statistical and Heuristic-Based Landslide Susceptibility Models: an Example from Ayvalık (Balıkesir, Northwestern Turkey). Journal of Geological Engineering 34 (2), 85-112.

Aleotti, P. & Chowdhury, R., 1999. *Landslide hazard assessment: summary review and new perspectives.* Bulletin of Engineering Geology and the Environment, 58, 21–44.

Atalay, İ., 1997. *Türkiye Coğrafyası*, Ege Üniversitesi Basımevi, ISBN 975-95527-5-2, Bornova, İzmir.

Ayalew, L., 1999. *The effect of seasonal rainfall on landslides in the highlands of Ethiopia*. Bulletin of Engineering Geology and The Environment. 58, 9–19.

Ayalew, L. & Yamagishi, H., 2005. *The application of GIS-based logistic regression for landslide susceptibility mapping in the Kakuda– Yahiko Mountains, central Japan*. Geomorphology, 65, 15–31.

Barredo, J.I., Benavides, A., Hervas, J. & Van Westen, C.J., 2000. *Comparing heuristic landslide hazard assessment techniques using GIS in the Trijana basin, Gran Canaria Island, Spain.* Journal of Applied Geodesy, 2(1), 9 – 23.

Boll, J., Brooks, E.S., Campbell, C.R., Stockle, C.O., Young, S.K., Hammel, J.E. & McDaniel, P.A., 1998. *Progress toward development of a GIS based water quality management tool for small rural watersheds: modification and application of a distributed model.* U.S. Army Corps of Engineers, 1960, Engineering and Design: Runoff from Snowmelt. EM 1110-2-1406.

Bonham-Carter, G.F., 1996. *Geographic Information Systems for Geoscientists, Modelling with GIS.* Pergamon Press, Canada.

Bresler, E., Russo, D., & Miller, R. D., 1978. *Rapid estimate of unsaturated hydraulic conductivity function.* Soil Science Society of America Journal, 42, 170–177.

Calcaterra, D., Parise, M., Palma, B. & Pelella, L., 2000. *The influence of meteoric events in triggering shallow landslides in pyroclastic deposits of Campania, Italy,* In: Proceedings 8th International Symposium on Landslides, (Bromhead E, Dixon N, Ibsen ML, eds), Cardiff: A.A. Balkema, 1, 209-214.

Can, T., Nefeslioglu, H.A., Gokceoglu, C., Sonmez, H. & Duman, T.Y., 2005. *Susceptibility assessments of shallow earthflows triggered by heavy rainfall at three subcatchments by logistic regression analyses*. Geomorphology, 72, 250–271.

Canoğlu, 2015. *An investigation on the surface water effect in landslide susceptibility mapping: an example from Yenice (Karabük) basin.* Institue of Science of Hacettepe University, PhD thesis, 140p.

Carrara, A., Cardinali, M., Detti, R., Guzzetti, F., Pasqui, V., & Reichenbach, P., 1991, *GIS techniques and statistical models in evaluating landslide hazard*. Earth Surface Processes and Landforms, 16(5), 427–445.

Carrara, A., Crosta, G. & Frattini, P., 2003. *Geomorphological and historical data in assessing landslide hazard.* Earth Surface Processes and Landforms, 28, 1125– 1142.

Çevik, E. & Topal, T., 2003. *GIS-based landslide susceptibility mapping for a problematic segment of the natural gas pipeline, Hendek (Turkey).* Environmental Geology, 44, 949–962.

Çevik, E. & Topal, T., 2004. *Relocation of a problematic segment of a natural gas pipeline using GIS-based landslide susceptibility mapping, Hendek (Turkey),* In: Hack R, Azzam R, Charlier R (eds) Proceedings of the 1st European Regional IAEG conference on engineering geology for infrastructure planning in Europe:a European Perspective, pp 265–274.

Clerici, A., Perego, S., Tellini, C. & Vescovi, P., 2002. *A procedure for landslide susceptibility zonation by the conditional analysis method.* Geomorphology, 48, 264–349.

Clerici, A., Perego, S., Tellini, C. & Vescovi, P., 2006. *A GIS-based automated procedure for landslide susceptibility mapping by the Conditional Analysis method: the Baganza valley case study (Italian Northern Apennines).* Environmental Geology, 50, 941–961.

Concha-Dimas, A., Campos-Vargas, M. & Lopez-Miguel, C., 2007. *Comparing heuristic and bivariate methods for refining landslide susceptibility maps in northern Mexico City.* Environmental and Engineering Geoscience, 8, 277–287.

Conoscenti, C., Di Maggio, C. & Rotigliano, E., 2008. *GIS analysis to assess landslide susceptibility in a fluvial basin of NW Sicily (Italy).* Geomorphology, 94, 325–339.

Crosta, G.B., Dal Negro, P. & Frattini, P., 2003. *Soil slips and debris flows on terraced slopes.* Natural Hazards and Earth System Science, 3, 31–42.

Cruden, D. M. & Varnes, D. J., 1996. *Landslide types and processes.* In: Turner AK, Schuster RL (eds) Landslides, Investigation and Mitigation, Transportation Research Board. Special Report 247. Washington D.C., US, 36–75.

Dahal, R. K., Hasegawa, S., Nonomura, A., Yamanaka, M., Dhakal, S. & Paudyal, P., 2008 (a). *Predictive modelling of rainfall-induced landslide hazard in the Lesser Himalaya of Nepal based on weights-of-evidence.* Geomorphology, 102, 496–510.

Dahal, R. K., Hasegawa, S., Nonomura, A., Yamanaka, M., Masuda, T. & Nishino, K., 2008 (b). *GIS-based weights-of-evidence modeling in small catchments for landslide susceptibility mapping.* Environmental Geology, 54, 311–324.

Dietrich,W. E. & Sitar, N., 1997. *Geoscience and geotechnical engineering aspects of debris flow hazard assessment, invited overview paper.* In: Chen, C.-L. (Ed.), Debris-Flow Hazards Mitigation: Mechanics, Prediction, and Assessment Proceedings of the 1st Int. Conf. ASCE, San Francisco, 656–676.

Ercanoğlu, M. & Gökçeoğlu, C., 2004. *Use of fuzzy relations to produce landslide susceptibility map of a landslide prone area (West Black Sea Region,*

Turkey). Engineering Geology. 75, 229–250.

Ercanoğlu, M., 2005. *Landslide Susceptibility Assessment of SE Bartın (West Black Sea region, Turkey) by artificial neural networks.* Natural Hazards and Earth System Science, 5, 979 - 992.

Ercanoğlu, M., Gökçeoğlu, C. & Van Asch, T. V. J., 2004. *Landslide Susceptiblity Zoning North of Yenice (NW Turkey) by Multivariate Statistical Techniques*. Natural Hazards, 32, 1 – 23.

Erdik, M., Üçer, B. & Barka, A., 1990. *Sinop nuclear power plant design basis ground motion.* General Directorate of Turkish Electricity Authority, Report No. 90-4.

Ertek, T. A., Turoğlu, H. & Mater, B., 1993. *Çiftlik Heyelanı (Sinop).* Türk Coğrafya Kurumu Dergisi, 181-188.

ESRI, Environmental Systems Research Institute, 2010.

Fernandez, T., Irigary, C., Hamdouni, R. E. & Chacon, J., 2003. *Methodology for landslide susceptibility mapping by means of a GIS. Application to the Contraviesa Area (Granada, Spain).* Natural Hazards, 30, 297–308.

Frey, M. P., Schneider, M. K., Dietzel, A., Reichert, P. & Stamm, C., 2009. *Predicting critical source areas for diffuse herbicide losses to surface waters: Role of connectivity and boundary conditions.* Journal of Hydrology, 365, 23–26.

Giannecchini, R., Galanti, Y. & D'Amato Avazi, G., 2012. *Critical rainfall thresholds for triggering shallow landslides in the Serchio River Valley (Tuscany, Italy).* Natural Hazards and Earth, System Science, 12, 829-842.

Gökçeoğlu, C. & Aksoy, H., 1996, *Landslide susceptibility mapping of the slopes in the residual soils of the Mengen region (Turkey) by deterministic stability analyses and image processing techniques.* Engineering Geology, 44, 147-161.

Gökçeoğlu, C., Sönmez, H., Nefeslioğlu, H. A., Duman, T. Y. & Can, T., 2005. *The March 17, 2005 Kuzulu landslide (Sivas, Turkey) and landslide susceptibility map of its close vicinity.* Engineering Geology, 81, 65–83.

Guzzetti, F., Cardinali, M., Reichenbach, P. & Carrara, A., 2000. *Comparing landslides maps: a case study in the Upper Tiberbasin, Central Italy.* Journal of Environmental Management, 25 (3), 247–263.

Gülkan, P., Yücemen, S., Koçyiğit, A., Doyuran, V. & Başöz, N., 1993. *En son verilere göre hazırlanan Türkiye Deprem Bölgeleri Haritası.* ODTÜ , Deprem Mühendisliği Araştırma Merkezi, Rapor No. 93-01 (unpublished report, in Turkish).

He, Y. P., Xie, H., Cui, P., Wei, F. Q., Zhong, D. L. & Gardner, J. S., 2003. *GIS based hazard mapping and zonation of debris flows in Xiaojiang Basin, Southwestern China.* Environmental Geology 45, 286–293.

Hutchinson, J.N., 1995. *Landslide hazard assessment*. Proc. 6th Symposium on Landslides, Christchurch, vol. 1, pp. 1805–1842.

Işık, N. S., Doyuran, V. & Ulusay, R., 2004. *Assessment of coastal landslide subjected to building loads at Sinop, Black Sea region, Turkey, and stabilization measures.* Engineering Geology, 75, 69-88.

Ives, J.D. & Messerli, B., 1981. *Mountain hazard mapping in Nepal: introduction to an applied mountain research project.* Mountain Research and Development, 1 (3–4), 223– 230.

Kim, J., Lee, K., Jeong, S. & Kim,G., 2014. *GIS based prediction method of landslide susceptibility using a rainfall infiltration-groundwater flow model.* Engineering Gology, 182, 63-78.

Kouli, M., Loupasakis, C., Soupios, P. & Vallianatos, F., 2010. *Landslide hazard zonation in high risk areas of Rethymno Prefecture, Crete Island, Greece.* Natural Hazards, 52, 599–621.

Kurtuluş, B. & Razack, M., 2010. *Modeling daily discharge of a large karstic aquifer using soft computing methods: Artificial neural network and neuro-fuzzy.* Journal of Hydrology, 381, (1-2), 101-111.

Kurtuluş, B., 2012. *High Resolution Numerical Modelling of SO_2 Emission: A Power Plant Case Study.* Building Simulation, 5, 135-146.

Kurtuluş, B., Flipo, N., 2012. *Hydraulic head interpolation using ANFIS—model selection and sensitivity analysis.* Computers and Geosciences, 38, 43–51.

Leroi, E., 1996. *Landslide hazard-risk maps at different scales: objectives, tools and developments.* In: Proc. VII. Int. Symp. Landslides, Trondheim, vol 1, pp. 35– 52.

Lin, M. L. & Tung, C. C., 2003. *A GIS-based potential analysis of the landslides induced by the Chi–Chi Earthquake.* Engineering Geology, 71, 63–77.

Magliulo, P, Di Lisio, A., Russo, F. & Zelano, A., 2008. *Geomorphology and landslide susceptibility assessment using GIS and bivariate statistics: a case study in southern Italy.* Natural Hazards, 47, 411–435.

Mathew, J., Jha, V. K. & Rawat, G. S., 2007. *Weights of evidence modelling for landslide hazard zonation mapping in part of Bhagirathi valley, Uttarakhand.* Current Science, 92, 628–638.

Montgomery, D. R. & Dietrich, W. E., 1994. *A physically based model for the topographic control on shallow landsliding.* Water Resources Research. 30, 1153–1171.

National Mapping Agency of Turkey, *1/25000 scaled Sinop E34-a1 topographic map*, 1993.

Özdemir, N., 2005. *Sinop ilinde etkili bir doğal afet türü heyelan*. D.Ü. Ziya Gökalp Eğitim Fakültesi Dergisi, 5, 67-106.

Pack, R.T., Tarboton, D.G. & Goodwin, C.N., 1998. *The SINMAP approach to terrain stability mapping*. In D.P. Moore & O. Hungr (eds.), Proceedings, Eighth International Congress of the International Association for Engineering Geology and the Environment. Vancouver, Canada, September 21-25, 1998: 1157 - 1165.

Rawls, W. J., Brakensiek, D. L., & Saxton, K.E., 1982. *Estimation of soil water properties.* Transactions of

the American Society of Agricultural Engineers, 25, 1316-1328.

Rawls, W., & D. Brakensiek, 1985. *Prediction of soil water properties for hydrologic modeling.* Watershed Management in the Eighties, 293–299.

Ray, R. L. & De Smedt, F., 2009. *Slope Stability Analysis using GIS on a Regional Scale: a case study from Dhading, Nepal.* Environmental Geology, 57(7), 1603–1611.

Ray, R. L., Jacobs, J. M. & Ballestero, T. P., 2011. *Regional landslide susceptibility: spatiotemporal variations under dynamic soil moisture conditions.* Natural Hazards 59, 1317–1337.

Ray, R. L., Jacobs, J. M. & Pedro de Alba, 2010. *Impacts of unsaturated zone soil moisture and groundwater table on slope instability.* Journal of Geotechnical and Geoenvironmental Engineering, 136, 1448 – 1458.

Rupke, J., Cammeraat, E., Seijmonsbergen, A.C. & Van Westen, C.J., 1988. *Engineering geomorphology of the Widentobel catchment, Switzerland: a geomorphological inventory system applied to geotechnical appraisal of the slope stability.* Engineering Geology, 26, 33 – 68.

Saha, A. K., Gupta, R. P., Sarkar, I., Arora, M. K. & Csaplovics, E., 2005. *An approach for GIS-based statistical landslide susceptibility zonation— with a case study in the Himalayas.* Landslides, 2, 61–69.

Skempton, A. W. & DeLory, F. A., 1957. *"Stability of natural slopes in London clay."* Proc., 4th Int. Conf. on Soil Mechanics and Foundation Engineering, Vol. 2, Butterworths Scientific Publications, London, 378–381.

Soeters, R. & van Westen, C.J., 1996. *Slope instability recognition analysis and zonation.* In: Turner K.T., Schuster, R.L. (eds.). Landslides: investigation and mitigation. Transportation Research Board National Reseacrh Council, Special Report No: 247, Washington, DC, 129 - 177.

Soil and Water Laboratory, 2003. SMDR – *The Soil Moisture Distribution and Routing model, version 2.0 – documentation.* Department of Biological and Environmental Engineering, Cornell University, Ithaca, New York. 88.

Süzen, M. L. & Doyuran, V., 2004(a). *A comparison of the GIS based landslide susceptibility assessment methods: multivariate versus bivariate.* Environmental Geology, 45, 665–679.

Süzen, M. L. & Doyuran, V., 2004 (b). *Data driven bivariate landslide susceptibility assessment using geographical information systems: a method and application to Asarsuyu catchment, Turkey.* Engineering Geology, 71, 303–321.

Süzen, M. L. & Kaya, B. K., 2012. *Evaluation of environmental parameters in logistic regression models for landslide susceptibility mapping.* International Journal of Digital Earth, 5 (4), 338 - 355.

USDA Soil Survey Staff, 1999. *Natural Resources Conservation Services, A Basic System of Soil Classification for Making and Interpreting Soil Surveys.* United States Department of Agriculture, second edition. 871.

Van Westen, C. J. & Terlien, T. J., 1996. *An approach towards deterministic landslide hazard analysis in GIS: a case study from Manizales (Colombia).* Earth Surface Processes and Landforms, 21,853–868.

Van Westen, C.J., Rengers, N. & Terlien, M.T.J., 1997. *Prediction of the occurrence of slope instability phenomena through GIS based hazard zonation.* International Journal of Earth Science, 86, 404– 414.

Varnes, D. J., 1984. *Landslide hazard zonation: a review of principles and practice, IAEG Commission on Landslides and other Mass Movements.* UNESCO Press, Paris, 63.

Wilcock, P. R., Schmidt, J. C., Wolman, M. G., Dietrich, W. E., Dominick, D. W., Doyle, M. W., Gordon, E. G., Iverson, R. M., Montgomery, D. R., Pierson, T. C., Schilling, S. P. & Wilson, R. C., 2003. *When models meet managers: examples from geomorphology.* In: Wilcock, P.R., Iverson, R.M. (Eds.), Prediction in Geomorphology, American Geophysical Union Monogragh Series 135, pp. 27–40.

Yalçın, A., 2008. *GIS-based landslide susceptibility mapping using analytical hierarchy process and bivariate statistics in Ardesen (Turkey): comparisons of results and confirmations. Catena* 1, 1–12.

Yeşilnacar, E. & Topal, T., 2005. *Landslide susceptibility mapping: A comparison of logistic regression and neural networks methods in a medium scale study, Hendek region (Turkey).* Engineering Geology, 79, 251-266.

Yılmaz, Ç., Topal, T. & Süzen, M. L., 2012. *GIS-based landslide susceptibility mapping using bivariate statistical analysis in Devrek (Zonguldak-Turkey),* Environmental Earth Science, 65 (7), 2161 - 2178.

Yılmaz, I. & Yildirim, M., 2006. *Structural and geomorphological aspects of the Kat landslides (Tokat-Turkey), and susceptibility mapping by means of GIS.* Environmental Geology, 50, 461–472.

Received at: 23. 04. 2016
Revised at: 17. 11. 2016
Accepted for publication at: 11. 01. 2017
Published online at: 07. 02. 2017